Picosecond photoelectric characteristic in La0.7Sr0.3MnO3/Si p-n junctions

Hui-Bin Lu, Kui-Juan Jin, Yan-Hong Huang, Meng He, Kun Zhao et al.

Citation: Appl. Phys. Lett. **86**, 241915 (2005); doi: 10.1063/1.1946901
View online: http://dx.doi.org/10.1063/1.1946901
View Table of Contents: http://apl.aip.org/resource/1/APPLAB/v86/i24
Published by the AIP Publishing LLC.

Picosecond photoelectric characteristic in $La_{0.7}Sr_{0.3}MnO_3$/Si *p-n* junctions

Hui-Bin Lu,[a] Kui-Juan Jin, Yan-Hong Huang, Meng He, Kun Zhao, Bo-Lin Cheng, Zheng-Hao Chen, Yue-Liang Zhou, Sou-Yu Dai, and Guo-Zhen Yang
Beijing National Laboratory for Condensed Matter Physics, Institute of Physics, Chinese Academy of Sciences, Beijing 100080, China

(Received 14 October 2004; accepted 4 May 2005; published online 9 June 2005)

Ultrafast photoelectric effects have been observed in $La_{0.7}Sr_{0.3}MnO_3$/Si *p-n* junctions fabricated by laser molecular-beam epitaxy. The rise time was ~210 ps and the full width at half-maximum was ~650 ps for the photovoltaic pulse when the junction was irradiated by a 1064 nm laser pulse of 25 ps duration. The photovoltaic sensitivity was as large as 435 mV/mJ for a 1064 nm laser pulse. No such photovoltaic signal was observed with irradiation from a 10.6 μm CO_2 laser pulse. The results reveal that this phenomenon is an ultrafast photoelectric effect. © *2005 American Institute of Physics*. [DOI: 10.1063/1.1946901]

Many efforts have been devoted recently to explore quantum functional properties and verify new device concepts based on manganese oxide. Tanaka *et al.* reported the electrical modulation of double-exchange ferromagnetism in $La_{0.9}Ba_{0.1}MnO_3$/Nb-doped $SrTiO_3$ *p-n* junction.[1] Mitra *et al.* observed a large positive magnetoresistance (MR) in a $La_{0.7}Ca_{0.3}MnO_3/SrTiO_3/La_{0.7}Ce_{0.3}MnO_3$ tunnel junction.[2] We have investigated the fabrication technology of atomically controlled oxide films on other oxides[3,4] and discovered the modulation effect of current and voltage as well as a large positive MR effect in systems of Sr-doped $LaMnO_3$ and Nb-doped $SrTiO_3$ *p-n* junctions[5,6] as well as multilayer *p-n* heterostructure.[7] With regard to optical effects on manganese oxides, Zhang *et al.* found laser-induced thermoelectric voltages in $La_{1-x}Ca_xMnO_3$ films with a photovoltaic pulse of ~2 μs full width at half-maximum (FWHM) when the film was irradiated by a 1064 nm laser pulse of 15 ns duration.[8] Sun *et al.* observed photovoltaic effect in $La_{0.29}Pr_{0.38}Ca_{0.33}MnO_3/SrNb_{0.005}Ti_{0.995}O_3$ *p-n* junction with a photovoltaic pulse of ~8 ms FWHM when the $La_{0.29}Pr_{0.38}Ca_{0.33}MnO_3$ film in the junction was irradiated by a 532 nm laser pulse of 10 ns duration.[9] In order to combine the functional properties of oxide with Si electronics, several insulating oxide films, such as $SrTiO_3$, $BaTiO_3$, and ferroelectric $Bi_{3.25}La_{0.75}TiO_{12}$ films, were reported to be epitaxially deposited on Si substrates.[10–12] In this letter, we present the laser molecular-beam epitaxy (laser MBE) and ultrafast photoelectric effect of $La_{0.7}Sr_{0.3}MnO_3$ (LSMO)/Si *p-n* junctions. The rise time was ~210 ps and FWHM was ~650 ps of the photovoltaic pulse when the LSMO film in the junction was irradiated by a 1064 nm laser pulse of 25 ps duration.

To form a *p-n* junction with functional properties by using an oxide and Si semiconductor, we chose LSMO as a *p*-type material, and 2 in. *n*-type Si (001) wafers with resistivity of 4 Ω cm as the substrates. The lattice mismatch between LSMO (~3.86 Å) and Si (5.43 Å) is fairly small [$\sim 0.55\% = (3.86\sqrt{2})/5.43$] with the LSMO unit cell rotated 45° around Si surface normal [100] axis. The LSMO films were fabricated by a computer-controlled (laser MBE).[3] Before depositing the LSMO film, Si substrates were carefully cleaned sequentially using alcohol, acetone, and deionized water. The substrates were then dipped into a ~5% HF solution for 20–30 s to remove the native silicon oxide on the surfaces and to form a hydrogen-terminated surface at the same time. Subsequently, the Si substrates were transferred into the epitaxial chamber immediately. When the base pressure of epitaxial chamber was pumped to 5×10^{-6} Pa, a focused pulsed XeCl excimer laser beam (~20 ns, 2 Hz, ~1.5 J/cm^2) was irradiated onto a hot-pressed LSMO target. The initial about 12 Å (~3 unit cells) LSMO film was deposited onto the Si substrate surface at room temperature to prevent the formation of the amorphous SiO_2 layer. The Si substrate was then raised to 620 °C in the base pressure of $\sim1\times10^{-5}$ Pa before the deposition of the LSMO film started again. An *in situ* reflection high-energy electron diffraction (RHEED) system and CCD camera was used to monitor the growth process of the LSMO thin films. The RHEED streak pattern of the LSMO film with the thickness of 12 Å appeared when the initial 12 Å LSMO film was crystallized by increasing the substrate temperature up to 620 °C and the thermal annealing process. The LSMO was continuously deposited and meanwhile an active oxygen source (~10% O) was introduced into the chamber and a pressure of 3×10^{-2} Pa was kept during the deposition. The thickness of the LSMO films of samples we deposited for the measurement were in the range of 300–600 nm. The crystallization of the LSMO film was examined *in situ* by RHEED, and also was characterized *ex situ* using x-ray diffraction (XRD) analysis.

The RHEED pattern of 400 nm LSMO film is shown in the inset of Fig. 1. The sharp streak pattern indicates that the LSMO film has a good crystallized structure and smooth surface. Figure 1 shows a typical XRD pattern of 400 nm LSMO film on Si substrate. Except for LSMO (001) and (002) and Si (002) diffraction peaks, there is no diffraction peak from impurity phases or randomly oriented grains, which implies that the LSMO film is *c*-axis oriented; that is, LSMO [110]$\|$Si[001].

To determine the electrical and photoelectric behaviors of the *p-n* junction, the 2 in. sample of LSMO/Si was cut into 5×6 mm^2 and 2×2 mm^2 for the photoelectric and electrical measurements. The indium (In) electrodes were placed on the surfaces of the LSMO thin films and Si substrates, as shown in the insets in Figs. 2, 3, and 4. For the

[a]Electronic mail: hblu@aphy.iphy.ac.cn

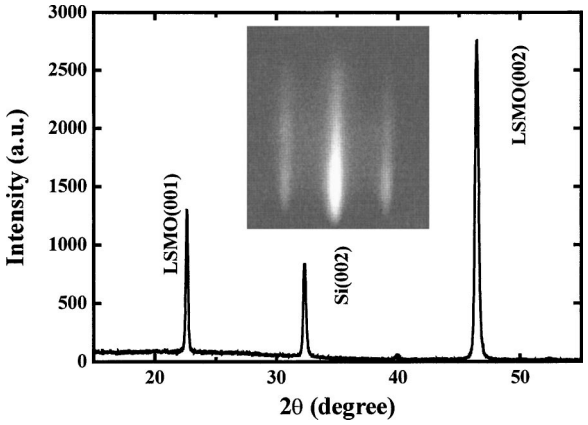

FIG. 1. A typical XRD pattern of 400 nm LSMO film on Si substrate. The inset is a RHEED pattern of 400 nm LSMO film on Si substrate.

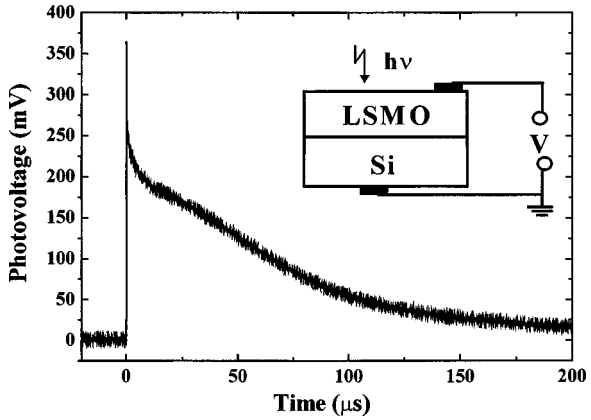

FIG. 3. Variation of the open-circuit photovoltage with time after excitation with a 1064 nm laser pulse on the LSMO/Si *p-n* junction. The schematic circuit of the sample measurement is shown in the inset.

photoelectric measurement, the In electrode was placed on a corner of the LSMO film surface.

The *I-V* characteristic of the LSMO/Si *p-n* junctions (2×2 mm^2) was measured with a pulse-modulated current source. Figure 2 shows an *I-V* curve of a LSMO/Si *p-n* junction at room temperature. The junction exhibits good nonlinear and rectifying *I-V* characteristics.

The photoelectric behaviors of LSMO/Si *p-n* junctions (5 mm$\times$6 mm) were further investigated using a 1064 nm Nd:YAG laser (pulse width 25 ps) as well as a 10.6 μm CO_2 pulse laser and measured by an oscilloscope of 130 ps rise time (Tektronix® TDS7254B) at ambient temperature. An open-circuit photovoltage to the *p-n* junction was observed between the two electrodes when the LSMO film surface was irradiated by a laser pulse. One of the most striking observations of the present work is the picosecond ultrafast photoelectric effect. Figure 3 shows the typical photovoltaic pulse as a function of time when the LSMO/Si *p-n* junction is irradiated with a 1064 nm laser pulse. The rise time is about 10 ns and the FWHM is about 12 μs when the photovoltage is directly measured. It should be noted that there is a sharp rise of the pulse at the very beginning, but then the photovoltage signal gradually decreases. When a 0.2 Ω resistance is connected in parallel with the *p-n* junction, as shown in Fig. 4, the rise time dramatically reduces to ~210 ps and the FWHM also reduces to ~650 ps. Evidently, the rise time and FWHM in Fig. 4 are much shorter than those in Fig. 3. The FWHM in Fig. 4 is about four orders of magnitude narrower than that of ~2 μs observed in Ref. 8, and about seven orders of magnitude narrower than that of ~8 ms observed in Ref. 9.

There are two main factors that influence the rise time and FWHM of the photovoltaic effect in Fig. 3. First, the interface of the *p-n* junction must be of good quality, as well as the LSMO film, because either defect at the interface or in the material would influence the production and lifetime of nonequilibrium carriers, which are of the same order as the decay time of the photovoltaic pulse in Fig. 3. Second, there is a junction capacitance in the LSMO/Si *p-n* junction as well as the impedance of the measurement system. In our case, the junction capacitance is about 30 pF at 500 MHz for the LSMO/Si sample of 5×6 mm^2, and the input impedance of the oscilloscope is 1 MΩ. In other words, the discharge time constant is about 30 μs, which is comparable to the FWHM of the photovoltaic pulse in Fig. 3, so it seems that the photovoltaic decay time in Fig. 3 is closely related to the *p-n* junction capacitance and the impedance in the measurement system. Therefore, the ultrafast photovoltaic pulse observed after connecting a 0.2 Ω resistance in parallel across the junction, as shown in Fig. 4, reveals a more realistic process of photoelectric emission in the *p-n* junction.

Our experimental results show that the photoelectric effect in the *p-n* junctions is not only an ultrafast effect, but is also highly sensitive to the laser pulse. The maximum photovoltaic sensitivity was 435 mV/mJ, and the maximum cur-

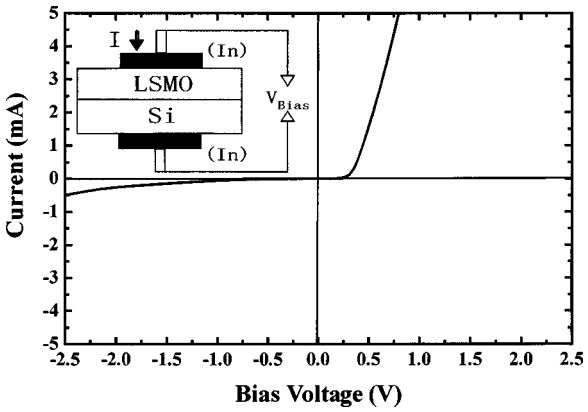

FIG. 2. *I-V* curve of a LSMO/Si *p-n* junction at room temperature. The schematic circuit of the sample measurement is shown in the inset.

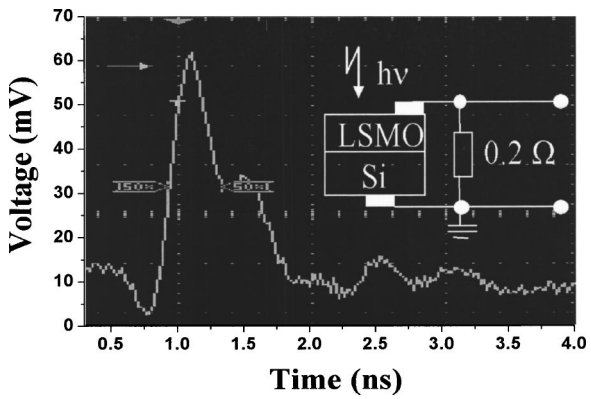

FIG. 4. Variation of the photovoltage with time under the same condition as in Fig. 3, but with a 0.2 Ω resistance connected in parallel across the *p-n* junction. Inset displays a schematic circuit of the sample measurement.

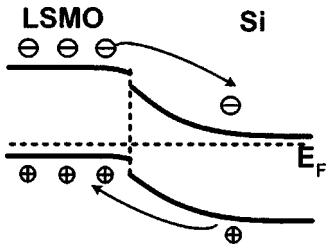

FIG. 5. Schematic band structure for the *p-n* junction of LSMO/Si, and the schematic movement of photon created carriers for the system irradiated by the laser pulse.

rents were more than 100 mA when a resistance $\leqslant 0.5\ \Omega$ was connected in parallel across the junction for a 1064 nm laser pulse of 0.8 mJ energy.

Figure 5 shows the schematic band structure for LSMO/Si *p-n* junction, and the schematic movement of photon-created carriers for the system irradiated by the laser pulse. The Hall effect we measured showed that the carrier density of LSMO is around 3×10^{18} cm^{-3}, which is much greater than that of *n*-type Si (around 1×10^{16} cm^{-3}); therefore, the depletion region in Si should be much thicker than that of LSMO, as shown in Fig. 5. The creation of the photovoltaic process can be easily understood as follows. When LSMO was connected with Si, electrons from *n*-type Si leaked out into the adjacent *p*-type LSMO, and holes in LSMO moved into Si due to the carrier diffusion. The diffusion barrier was then built up around the interface to prevent the further leaking of carriers, meanwhile the potential of LSMO was raised by the space charge in the interface. With the radiation of photons, electrons in the valence band absorbed photons and transited to the conduction band. As the photon energy of 1064 nm wavelength is slightly larger than the band gaps of LSMO (1.0–1.3 eV) and Si ($\approx$1.12 eV), so the electrons and holes in LSMO and Si were created in the system. The created electrons with higher potential in LSMO side then flowed to the Si side, where the potential was lower. Meanwhile, holes in Si side should move to the LSMO side. After these movements, the Fermi level in Si was split into two quasi-Fermi levels during illumination. Eventually, the photovoltage occurred in the system. By doing the photon absorption measurement both for Si substrate and for LSMO/Si, we can conclude that photons (1064 nm wavelength) are absorbed mostly by LSMO rather than by Si. One possible reason could be that the heterostructure was illuminated from LSMO side by laser and the LSMO film is quite thick (400 nm). Therefore, the laser-induced carriers in the system are created mostly in LSMO film.

We did not observe any photoelectric effect when the LSMO film in the junction was irradiated by a 10.6 μm CO_2 laser pulse for which the photon energy is much smaller than either of the band gap of the LSMO or Si. This result clearly demonstrates that the ultrafast photovoltage is a photoelectric effect instead of a thermoelectric effect.

In conclusion, we have fabricated the LSMO/Si *p-n* junctions and observed the ultrafast photoelectric effects in the junctions. It is noteworthy that the *p-n* junction of LSMO and Si combine the functional properties of oxide with Si electronics. The key advantages of LSMO/Si is that the new structure consisting of a manganite as a MR material (LSMO) and a conventional semiconductor (Si) combines multifunction of MR,[13] rectification, and ultrafast photoelectric characteristic, which is with potential of new applications. The interesting properties of such a new structure related to spin ordering, charge carrying, and electron-photon interaction in the system are stimulating a widely study. Further investigation, both experimental and theoretical, on the mechanism of the multifunctional properties of electricity and optics and magnetics in such systems are under going.

The authors thank Dr. Wenhao Zhou and Dr. Yue Xu for their help in picosecond measurement, and Prof. R. Q. Tan for his help in CO_2 pulse laser. This work was supported by the National Natural Science Foundation of China (No. 10334070).

[1] H. Tanaka, J. Zhang, and T. Kawai, Phys. Rev. Lett. **88**, 027204 (2002).
[2] C. Mitra, P. Raychaudhun, K. Dorr, K. H. Muller, L. Schultz, P. M. Oppeneer, and S. Wirth, Phys. Rev. Lett. **90**, 017202 (2003).
[3] G. Z. Yang, H. B. Lu, F. Chen, T. Zhao, and Z. H. Chen, J. Cryst. Growth **227–228**, 929 (2001).
[4] N. Wang, H. B. Lu, W. Z. Chen, T. Zhao, F. Chen, H. Y. Peng, S. T. Lee, and G. Z. Yang, Appl. Phys. Lett. **75**, 3464 (1999).
[5] H. B. Lu, S. Y. Dai, Z. H. Chen, L. Yan, Y. L. Zhou, and G. Z. Yang, Chin. Sci. Bull. **48**, 1016 (2003).
[6] H. B. Lu, S. Y. Dai, Z. H. Chen, L. F. Liu, H. Z. Guo, W. F. Xiang, Y. Y. Fei, M. He, Y. L. Zhou, and G. Z. Yang, Chin. Phys. Lett. **20**, 137 (2003).
[7] H. B. Lu, G. Z. Yang, Z. H. Chen, S. Y. Dai, Y. L. Zhou, K. J. Jin, B. L. Cheng, M. He, L. F. Liu, H. Z. Guo, Y. Y. Fei, W. F. Xiang, and L. Yan, Appl. Phys. Lett. **84**, 5007 (2004).
[8] P. X. Zhang, W. K. Lee, and G. Y. Zhang, Appl. Phys. Lett. **81**, 4026 (2002).
[9] J. R. Sun, C. M. Xiong, B. G. Shen, P. Y. Wang, and Y. X. Weng, Appl. Phys. Lett. **84**, 2611 (2004).
[10] K. Eisenbeiser, J. M. Finder, Z. Yu, J. Ramdani, J. A. Curless, J. A. Hallmark, R. Droopad, W. J. Ooms, S. Bradshaw, and C. D. Overgaard, Appl. Phys. Lett. **76**, 1324 (2000).
[11] R. A. Mckee, F. J. Walker, and M. F. Chisholm, Phys. Rev. Lett. **81**, 3014 (1998); Science **293**, 468 (2001).
[12] H. N. Lee, D. Hesse, N. Zakharov, U. Gosele, Science **296**, 2006 (2002).
[13] H. B. Lu, K. J. Jin, Y. H. Huang, M. He, K. Zhao, Z. H. Chen, Y. L. Zhou, and G. Z. Yang (unpublished).